TO:
FROM: Al Cooper
SUBJECT: Studies of the measurements of wind using LAMS

Introduction

During the 2015 ARISTO project on the C-130, the LAMS was flown in a 4-beam configuration. The beam assignments were non-standard, though, with beam 2 forward, beam 1 downward, beam 3 outboard and upward, and beam 4 inboard and upward. Beams 1, 3 and 4 were approximately 35° from the forward direction, and relative to an azimuthal angle starting from the downward direction they were, respectively, 0, −120 and 120° in clockwise rotation about the forward longitudinal axis.

There were five research flights. All had some degree of measurement problems, so data for this study have been selected from the periods that appear to provide the best measurements. The following table provides a few of the characteristics of these flights:

date	start	end	profile	problems
150916	160225	200605	climb->20kft, level, stepped descent to BL, no maneuvers	LAMS IRU attitude angles bad
150923	135907	204016	mostly low level until near end; LAMS reasonable, although weak; some speed variations	actual takeoff about 170000; BEAM2speed weak, BEAM2_LAMS (Scott's value) better.
150925	162500	214500	both upper and lower-level legs; speed runs, some turbulence	CPITCH_LAMS bad before 192300, and CROLL also, so wind measurements from LAMS unavailable until after then.
150930	170100	205000	good pitch and yaw maneuvers; also a partial speed run.	Beams 1 and 4 problematic before 1915 in high-level leg; beam 2 probably useful for TAS.
151002	143000	184400	upper-level pitches and lower-level turbulence	LAMS beam peaks look very weak to me, questionable although SMS processing seems reasonable.

The line-of-sight beam speeds were determined in two ways. Scott Spuler used principal-component analysis to find the beam speeds, and usually this worked very well, although there are some suspicious times. For example, the peaks in Flight 5 look very weak, yet the PCA method continued

to find output values. Because there was tight coupling to the expected measured TAS (with adjustment for the beam angles), it appears suspicious that the method may be duplicating the TAS value at times without having an adequate signal. The match to TASX looks so good that it seems suspicious, as discussed later. A second method was to fit the background using Savitzgy-Golay polynomials and then search for peaks above this background. When signals were strong, the method usually produced the same result as the PCA method, but it was more prone to failure during periods where the signal was weak. (A signal-to-noise test of ≥ 4 was required for a valid measurement.) Results from both these peak-detecting algorithms will be discussed in this memo.

There are several objectives that can be met by using the LAMS-derived measurements:

1. The LAMS provides an independent measurement of angle-of-attack and sideslip angle, so these measurements can be used to check the empirical relationships used to calibrate the radome-based measurements of these angles.

2. LAMS provides an independent measurement of the airspeed, so from that measurement it is possible to determine the expected dynamic pressure. This was used previously(Cooper et al., 2014) to calibrate not only the dynamic pressure but also the static pressure as measured on the C-130. However, since then the offset between the avionic static pressure and the research static pressure calibrated in this way has changed, so it is important to learn if the static defect actually changed or perhaps the avionic value changed. This has an important effect on the longitudinal component of the measured wind as well.

3. The paper by Cooper et al. (2014) developed a method for measuring temperature using the LAMS, which might have potential to provide a valid measurement of temperature in clouds. However, only a small sample of measurements were available, so it will be useful to explore if further measurements from ARISTO-2015 help characterize this measurement.

4. The method used to calibrate the radome is based primarily on slowly varying measurements, such as the variation in angle-of-attack during a speed run. It is of concern that the calibration used might not apply in the case of rapidly changing flight conditions, when for example there might be transient adjustment of the airflow pattern toward a new steady state. Because the LAMS measures wind well ahead of the aircraft, such effects should not appear in the LAMS-based measurements, so a comparison of the LAMS-based and radome-based measurements might either identify transient-response problems or place limits on how large such effects might be.

Data processing

The original netCDF files, with names like ARISTOrf01.nc, contain histograms of the LAMS frequency measurements, with names like BEAM{1–4}_LAMS. Scott Spuler has processed these to produce files like ARISTOrf01_LAMS.nc with new variables Beam{1–4}_LAMS containing the line-of-sight speeds measured in each beam. In addition, the Python program LAMS_ARISTO.py

has been used to process these further to files ARISTOrfxx_LAMSLAMS.nc, which contain additional variables BEAM{1–4}speed also representing the line-of-sight speeds. Both sets of variables, Beam{1–4}_LAMS and BEAM{1–4}speed, will be used, but they appear to have different strengths:

1. The variables Beam{1–4}_LAMS are produced by Spuler's PCA routine. This is the most sensitive detection method, but there is some suspicion that it produces values when there is inadequate signal, perhaps by too much reliance on TASX to determine where the peak should be.

2. The variables BEAM{1–4}speed are produced by smoothing the histograms with Savitzgy-Golay polynomials and then searching for peaks above the smoothed background. This algorithm also uses TASX to determine likely locations for the peaks, but with a fairly large tolerance, and it requires a signal-to-noise ratio ≥ 4 or else it produces a missing-value result. In ARISTO2015, this algorithm was significantly less sensitive than the PCA algorithm, and for example in Flight 5 it mostly did not produce useful results while the PCA algorithm produced almost continuous results for the line-of-sight beam speeds.

The Python routine also produced new variables named WD_LAMS, WS_LAMS, WI_LAMS, ATTACK_L and SSLIP_L, using the processing algorithms for a 4-beam LAMS that were discussed in the documents LAMSprocessing4Bwind.pdf and LAMSprocessing3Dwind.pdf. These variables were also used in the present R routine (this file) to generate measurements of vertical and horizontal wind, airspeed, and angles of attack and sideslip. For airspeed, angle of attack, and sideslip, these steps were used:

1. The four-beam measurements were used to determine a three-dimensional relative wind vector **RW**=$\{\mathrm{RW}_x, \mathrm{RW}_y, \mathrm{RW}_z\}$ with components inbound along the longitudinal forward, lateral starboard, and lateral downward axis in the coordinate frame of the LAMS IRU (with attitude angles CPITCH, CROLL, CTHDG). The algorithm is documented in LAMSprocessing4Bwind.pdf.

2. The airspeed is then the magnitude of the vector **RW**.

3. The angle of attack is $\alpha = \arctan(\mathrm{RW}_z/\mathrm{RW}_x)$ and the sideslip angle is $\beta = \arctan(\mathrm{RW}_y/\mathrm{RW}_x)$.

The results for the various processing schemes are shown in Fig. 1.

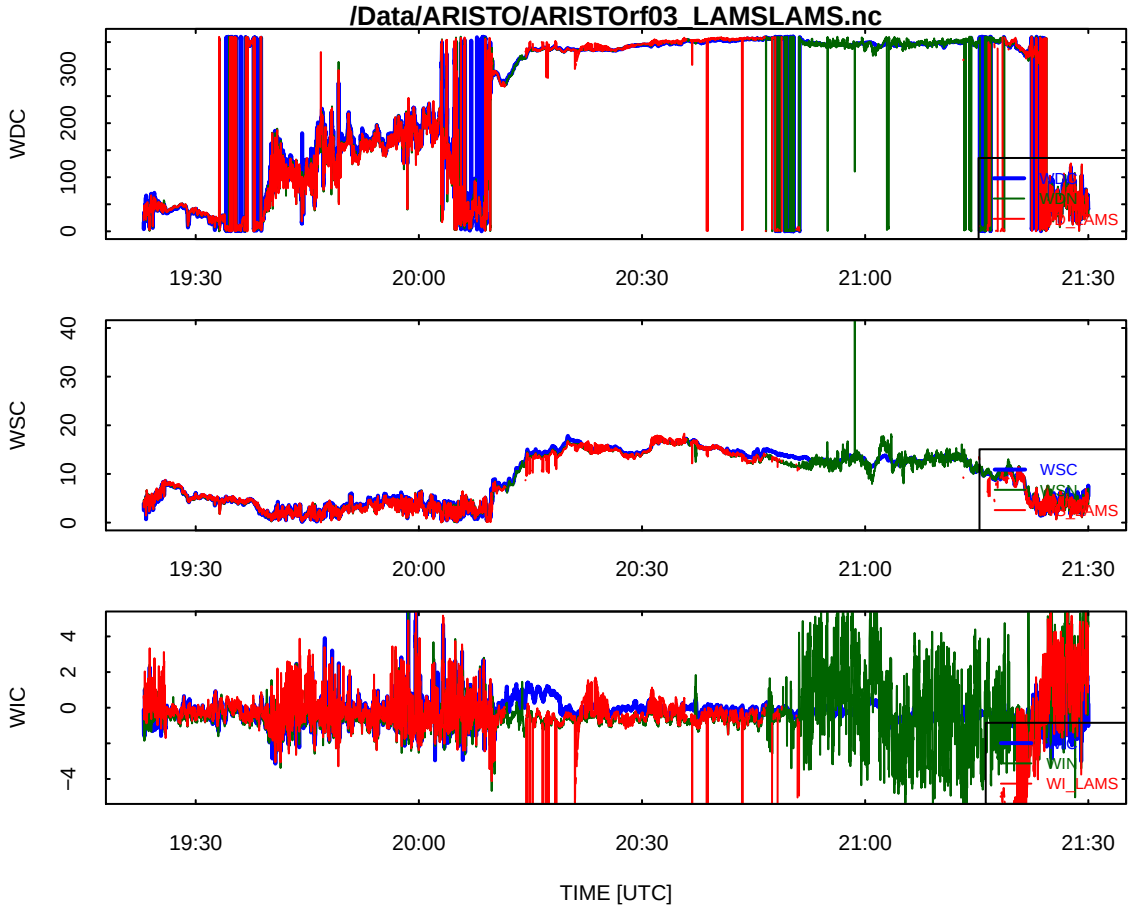

Figure 1: Wind measurements: conventional (blue), PCA-based (green), SG-based (red). The time period is restricted to 19:23–21:30 UTC because the LAMS IRU produced erronous values for the attitude angles at other times.

Sensitivity coefficients

Angle of attack

The following speed-run maneuvers are available from ARISTO2015:

#	flight	start	end	comments
1	2	183200	185500	PCA, not SG
2	2	192100	193800	PCA or (SG exc 193000)
3	3	171300	173800	CPITCH bad
4	3	183400	185700	CPITCH bad
5	3	205500	210000	slowdown only; PCA only
6	4	174300	180700	PCA only
7	4	191200	193000	PCA only; SG weak
8	4	202500	203900	PCA; SG B1 weak

The values of vertical wind as originally processed did not look very good, so the first step was to determine a conventional set of sensitivity coefficients to use as a radome calibration. For this purpose, a data.frame consisting of a concatenation of the eight speed runs in the preceding table was constructed and a reference value for calibration (AOAREF) was added to the data.frame. AOAREF, defined below, is the value that should be measured for angle of attack if the true vertical wind is zero during the maneuver:

$$\mathrm{AOAREF} = \theta + \frac{w_p}{V}\frac{180}{\pi}$$

where θ is the pitch angle (variable PITCH), w_p is the rate of climb of the aircraft (variable GGVSPD), and V is the true airspeed (variable TASX). The conventional fit is then

$$\mathrm{AOAREF} = c_0 + \frac{\mathrm{ADIFR}}{\mathrm{QCF}}\left(c_1 + c_2\,\mathrm{MACH}\right)$$

where MACH is the Mach number determined from the uncorrected measurements PSFD and QCF (cf. the technical note on processing algorithms). In addition, a data.frame consisting of all measurements from flights 2–4 was constructed and coefficients were also determined for a fit to those data.

Figure 2 shows the resulting fit, with coefficients $\{c_0, c_1, c_2\}$ = {4.7314, 11.5015, 3.0546}. However, the results differed for the three flights, and the differences were significant, as shown in the following table:

Flight	c_0	c_1	c_2
speed runs	4.7314	11.5015	3.0546
all rf02–04	4.6298	11.7147	1.5477
2	4.1623	6.0555	13.9073
3	4.5892	8.4874	8.5789
4	4.9885	12.4355	2.0626

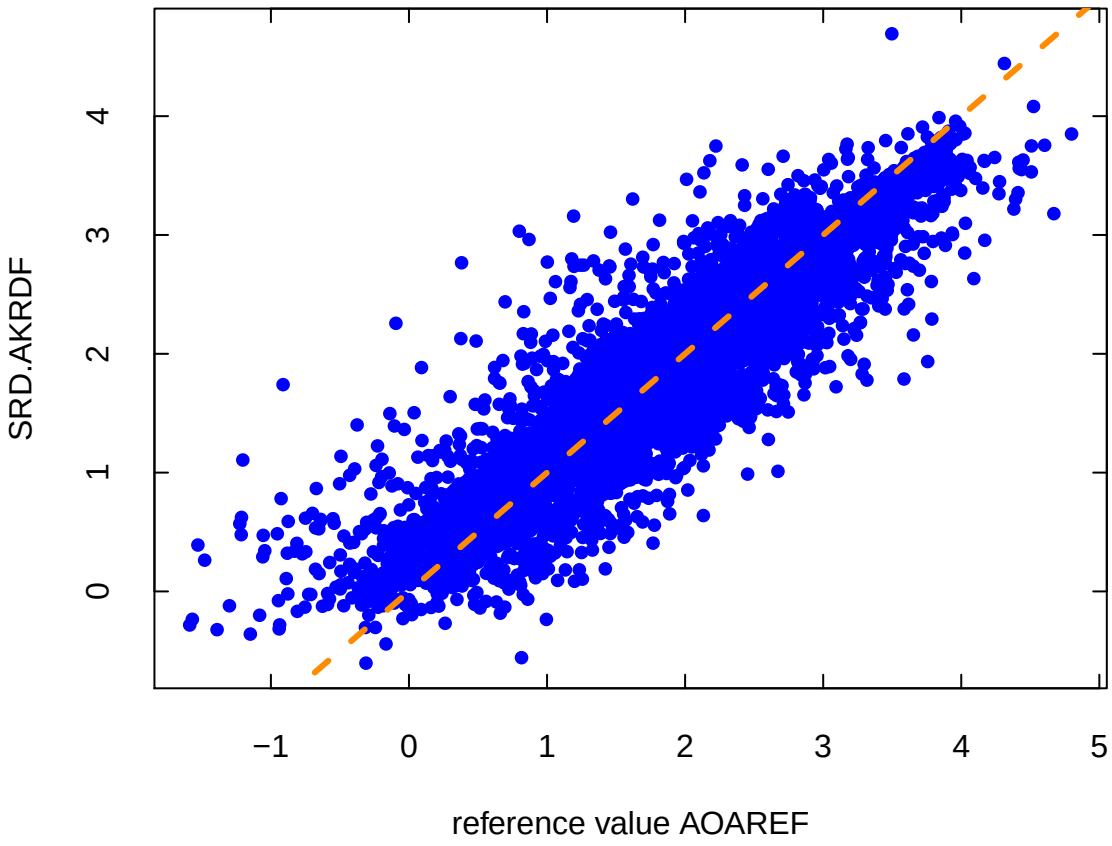

Figure 2: Angle of attack from the new calibration vs. the corresponding value of the reference variable AOAREF.

Therefore, the individual-flight coefficients will be used to determine AKRD and hence WIC in the following studies in this report.

An additional adjustment of the measurements is useful because the LAMS is not installed parallel to the centerline of the aircraft. For example, the average measurement of pitch from the LAMS IRU, CPITCH_LAMS, is 1.0° larger than the corresponding measurement of pitch from the Honeywell IRU. To account for this offset, it is useful to correct both the pitch and angle-of-attack from LAMS by the subtraction of 1.0° so that the measurements will be comparable to those from the standard radome-based system. That correction has been made in the following when the LAMS-based angle-of-attack is discussed.

With these corrections, the standard angle-of-attack can be compared to that determined from the LAMS. The first speed run in the table above will be skipped here because there are too many bad measurements from LAMS. For the second speed run, Figure 3 shows the comparison of the two angles of attack. There is a clear difference between the two measurements. Speed runs #3 and #5

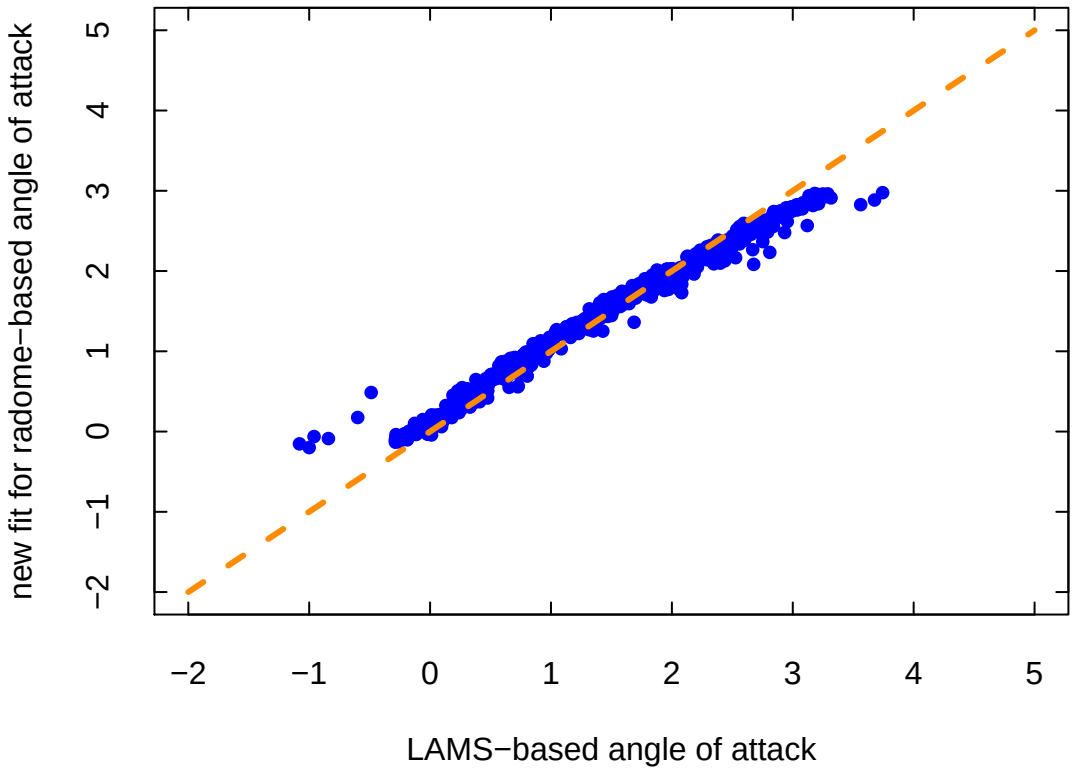

Figure 3: Angle of attack from the new fit to the radome values, plotted against the corresponding anagle-of-attack as measured by the LAMS, for speed run #2.

have too much scatter in the LAMS measurements to be useful, but speed run #4 has apparently good measurements as shown in Fig. 4. Here the scatter is much higher than in Fig. 3 because this is a low-level flight segment in boundary-layer turbulence, but the measurements still show an offset like that in Fig. 3, although perhaps with a smaller offset. Speed runs #6 and #8 have high scatter and are inconsistent with other apparently good speed runs, but speed run #7 led to good agreement between the values of the radome-based and LAMS-based angles of attack, as shown in Fig. 5.

Figures 3 and 5 show reasonable consistency between the two measurements, while there is a significant offset evident in Fig. 4. Because speed run #4 is a low-level boundary-layer leg, there may be bias introduced by the proximity of the ground and strong reflection from it that could affect the downward-pointing beam. A fit to the radome-based angle of attack as a function of the LAMS-based value gave regression coefficients of 0.66 (offset) and 0.70 (slope), so these measurements are clearly inconsistent.

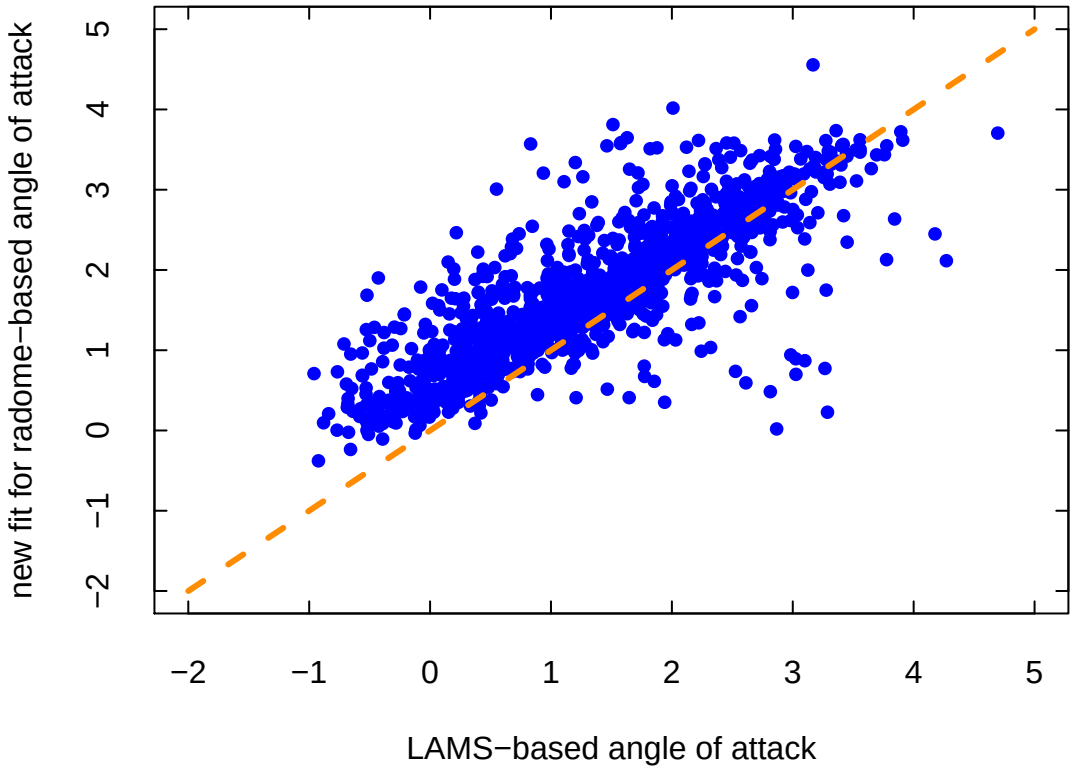

Figure 4: Angle of attack from the new fit to the radome values, plotted against the corresponding anagle-of-attack as measured by the LAMS, for speed run #4.

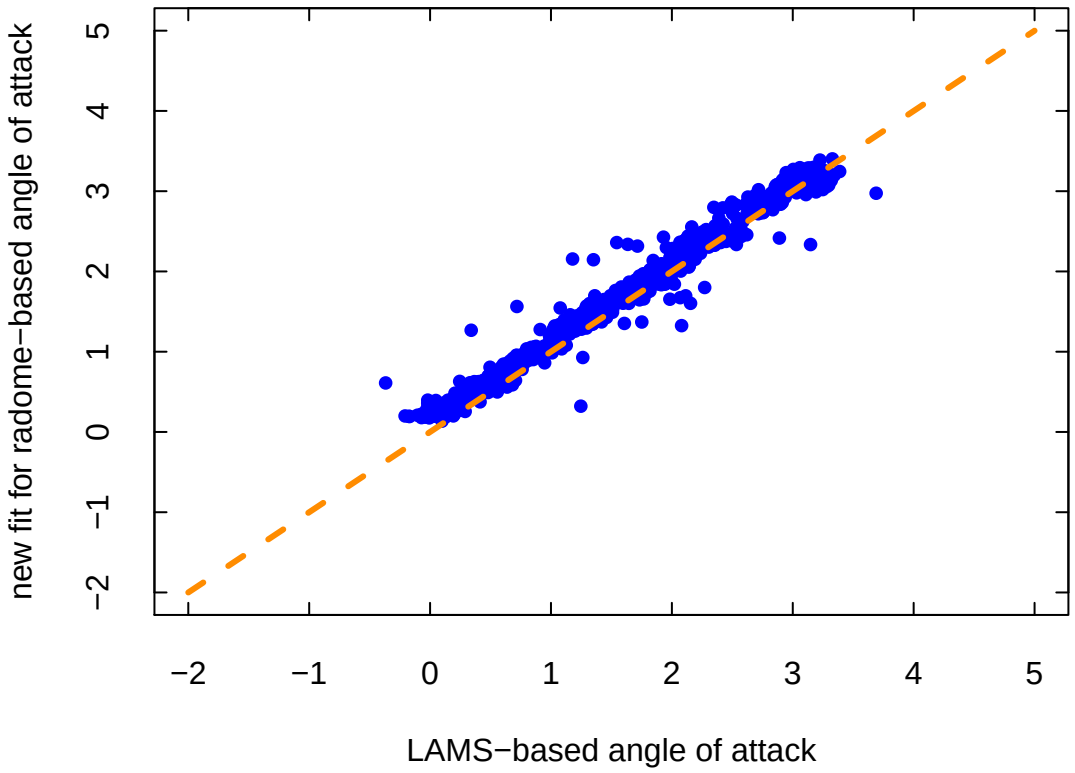

Figure 5: Angle of attack from the new fit to the radome values, plotted against the corresponding anagle-of-attack as measured by the LAMS, for speed run #7. Some additional outlier points having difference between the measurements larger than 1 degree have been excluded from the plot.

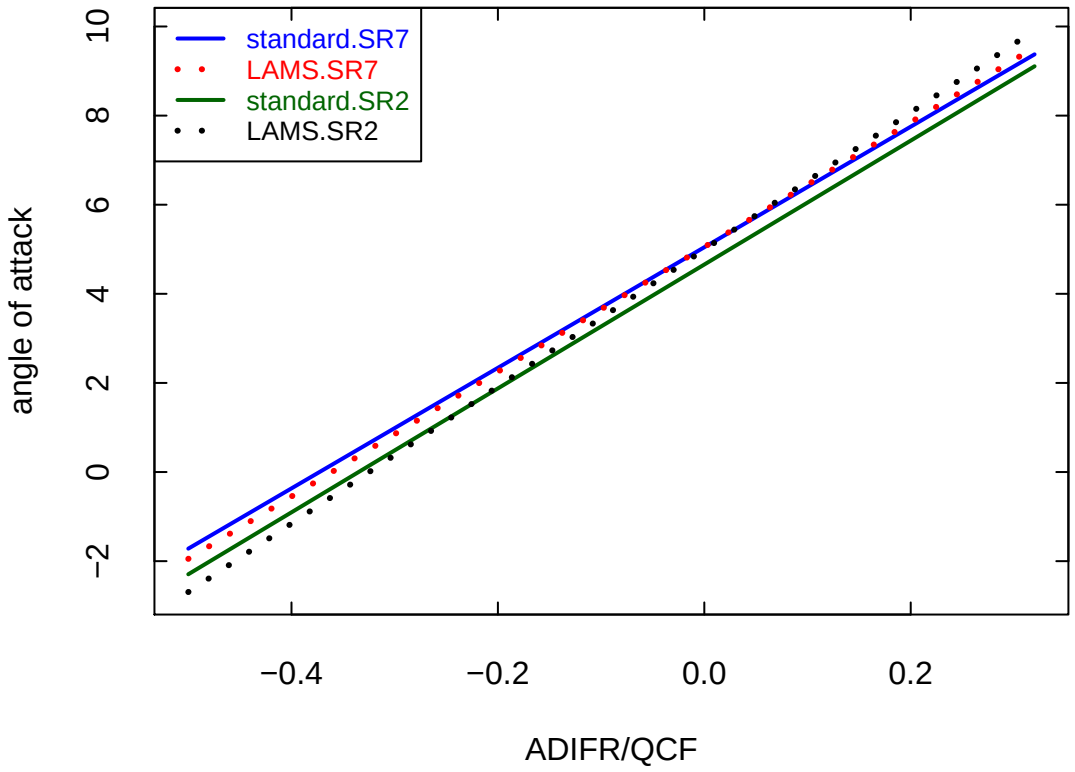

Figure 6: Comparison of the standard and LAMS-based calibrations for speed run #7.

A revised LAMS-based calibration for the radome sensitivity coefficients can then be determined by using the LAMS-based angle of attack as the reference for the fits. Separate fits for speed-run #2 and for #7 produced significantly different results, so both the conventional and LAMS-based calibrations differ for the two speed runs. The following table summarizes the results:

speed run	**source of calibration**	c_0	c_1	c_2
#2	AOAREF	4.6576	13.9045	0
#2	LAMS ATTACK	4.9945	15.3775	0
#7	AOAREF	5.0451	13.5299	0
#7	LAMS ATTACK	5.0512	13.9997	0
#2+#7	LAMS ATTACK	4.6694	9.7585	8.4181

The four calibrations in the preceding table are plotted in Fig. 6. For speed run #7, the calibrations based on LAMS and on AOAREF are close to the same, although there are small differences of typical magnitude of about 0.1°for angles-of-attack in the typical range of operations (0–4°).

However, the different calibrations for speed run #2 are not as consistent, and both calibrations differ significantly from those for speed run #7. A fit to the combined data from #2 and #7 is also shown for the LAMS calibration, but this fit was much worse than the individual-flight calibrations and showed two distinct lines with little overlap for the two plots, so this is not a good calibration to use for these flights. For the conventional calibration, the differencemight be attributed to a non-zero vertical wind during the calibration maneuver, but the LAMS calibration is not affected by the vertical wind so it should be definitive unless there was some problem with detection of the LAMS beams. Other possibilities are drift of the CPITCH_LAMS measurement or differences in altitude or Mach number. However, the difference between PITCH and CPITCH_LAMS is the same for speed run #2 as for speed run #7 and both were flown at almost the same altitude and range in Mach number, so these explanations appear to be ruled out.

The result is that the two best speed runs, #2 and #7, are inconsistent. Calibrations for speed run #7 support the validity of each, but there is larger than expected difference between the two calibrations for #2 and between the corresponding calibrations for #7 vs #2. These are the best calibration data available, so more measurements with adequate LAMS signal-to-noise would be valuable. Pending such measurements, the LAMS-based calibration for #7 may be the most reliable.

Another conclusion from the study of the speed runs is that the PCA analysis does not always produce reliable line-of-sight speeds. A good example is speed run #6. There are values for all four beam line-of-sight speeds through this maneuver, and the speed in the forward beam (Beam 2) matches the true airspeed (TASX) well. However, Fig. 7 shows that the angle-of-attack determined from these measurements does not match that determined from the radome-based system and looks very noisy. This raises a warning that sometimes the line-of-sight speeds are not valid even when the PCA algorithm detects peak values.

Sideslip angle

There were four yaw maneuvers that can be used to find the sensitivity coefficients for the sideslip measurement, as listed in the following table:

maneuver #	flight	start	end
1	2	194100	194330
2	4	182800	183100
3	4	190130	190400
4	4	201830	202130

First, for completeness, the conventional fit will be used:

$$\beta^* = -\Psi + \arctan\frac{u_p - u}{v_p - v}$$

where β^* is the reference value for the fit, Ψ is the heading, u_p and v_p the eastward and northward components of the aircraft ground-speed and u and v are the east and north components of

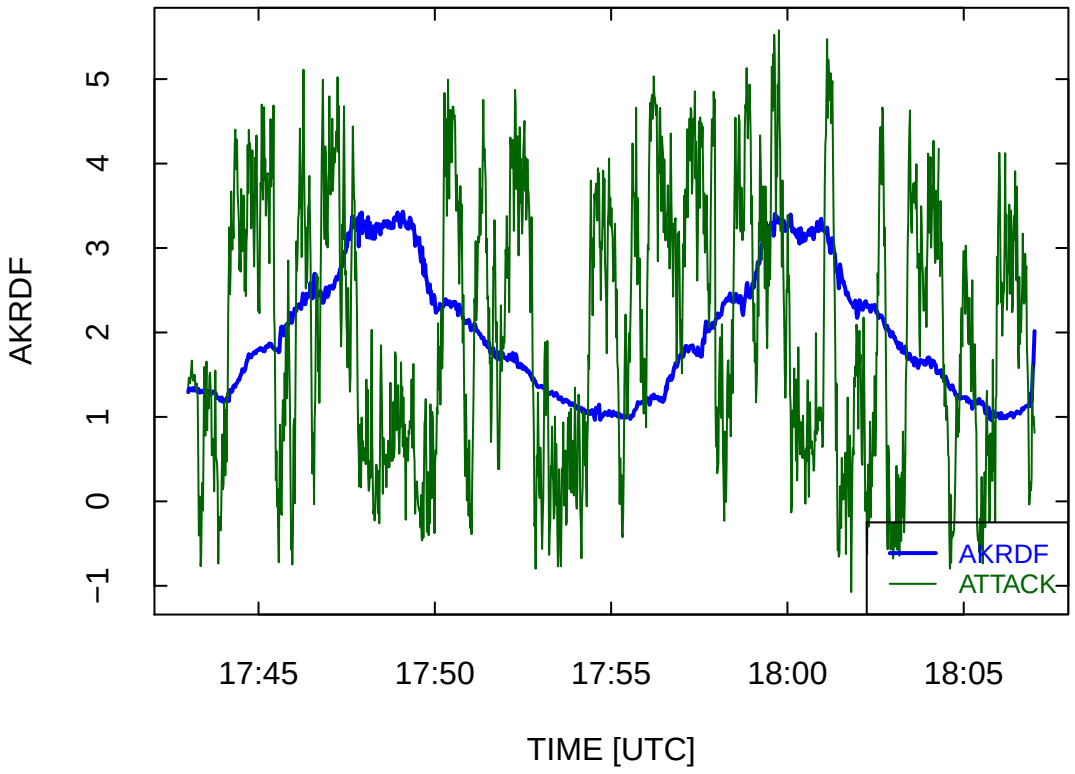

Figure 7: Angle of attack from the new fit to the radome values (blue line) and the angle-of-attack determined from the LAMS measurements (green line), for speed run #6.

the wind. The empirical relationship for sideslip then can be found by fitting for the coefficients $\{s_0, s_1\}$ in:

$$\beta^* = b_0 + b_1 \frac{\text{BDIFR}}{\text{QCXC}}$$

and then finding the sideslip angle from

$$\text{SSRD} = b_0 + b_1 \frac{\text{BDIFR}}{\text{QCXC}} \ .$$

Figure 8 shows that the resulting values for SSRD are in close correspondence to the reference values for the four combined yaw maneuvers.

The resulting sensitivity coefficients for sideslip are $\{b_0, b_1\}$ = {1.5478, 12.6582}. The fit was very good, with a residual standard deviation of 0.12°. For comparison, the standard values in the

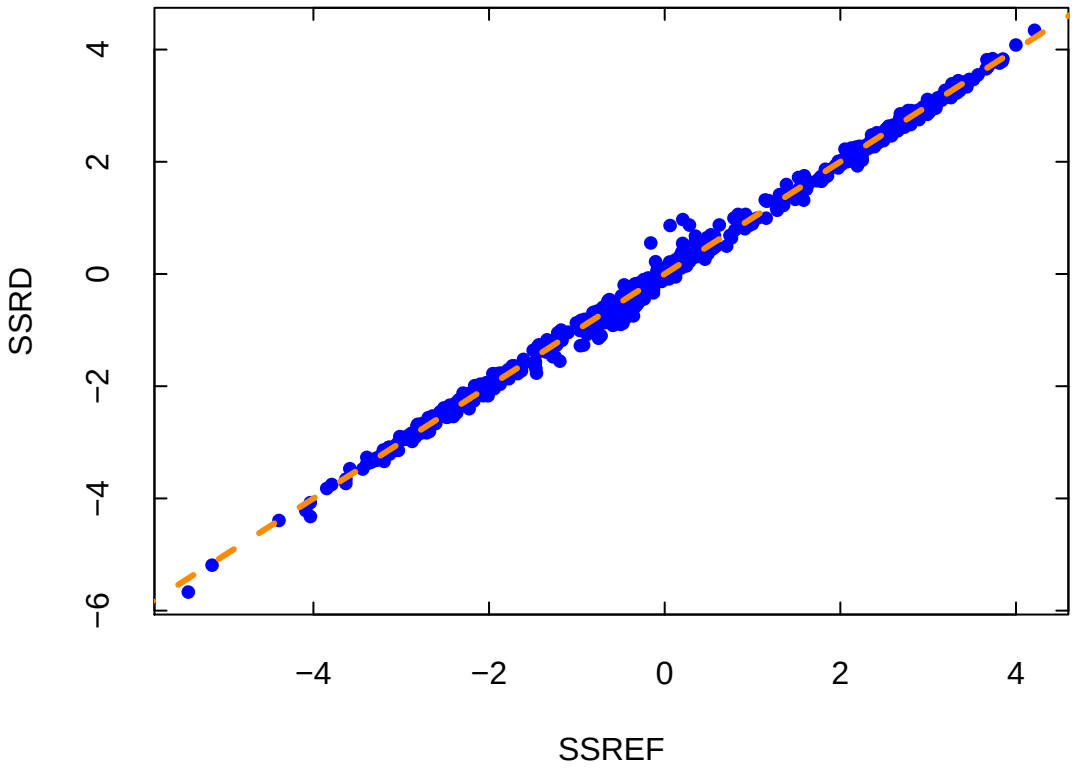

Figure 8: Sideslip angle calculated using new fit coefficients (SSRD) as a function of the reference value for sideslip (SSREF). The relationship determined by regression is shown as the dashed orange line.

Technical Note on Processing Algorithms are {0, 12.2115}. As discussed in the Technical Note on Wind Uncertainty, it is difficult to separate an offset in sideslip from an offset in heading, so the difference in the first coefficient may instead apply to heading.[1] The difference in offsets for these two calibrations is large, although the slope coefficients are in reasonable agreement.

The LAMS measurement of sideslip provides an alternate means of determining the slope parameter.[2] The reference value β^* for the fit can be determined from the LAMS-based measurements of the relative wind, as discussed in the introductory section:

$$\beta^* = \arctan\left(\frac{\mathrm{RW}_y}{\mathrm{RW}_x}\right)$$

[1] An offset of -0.1° applied to heading in the original processing has not been removed here.
[2] The appropriate offsets in sideslip and heading will still need to be found from analysis of circle maneuvers.

The LAMS-based measurements of sideslip bear little similarity to those from the radome for sideslip maneuvers #2 and #3, so there are evidently measurement problems that make those unreliable. Maneuver #4 is good, and maneuver #1 appears valid for the period 194130–194305, so those measurements were used for the fit. The LAMS-based fit gave coefficients $\{b_0, b_1\} = \{1.5995, 12.3612\}$, with a residual standard deviation about the fit of 0.13°. These values are close to those determined in the standard way, so this calibration provides support for the conventional approach, although the difference in slope is significant (with estimated standard uncertainty in b_1 of 0.05°). The value for b_1 determined from the LAMS-based measurements, 12.36°, appears to be the best available, but the value of b_0 still needs to be determined from the circle maneuvers that can separate an offset in sideslip from an offset in heading.

Calibration of the pressure defect

A previous calibration of the C-130 pressure defect was published in Cooper et al., 2014. The key to this calibration is that LAMS provides a measurement of airspeed, from which the dynamic pressure can be calculated if the temperature and pressure are known. The result is relatively insensitive to temperature and pressure, so this is an accurate result despite the need to know the airspeed to calculate the temperature and the need to know the static defect to calculate the pressure. Because a pitot tube is thought to provide a valid measurement of the total pressure, subtracting the dynamic pressure from the total pressure gives the true ambient pressure. The difference between this value and the measured pressure is then the static defect. Furthermore, because the measured dynamic pressure is based on a measurement of the difference between the total and static pressures, the same correction represented by the static defect applies with reversed sign to the measured dynamic pressure.

The equation published there, Eq. 11, was subsequently revised to avoid circularity in data processing by basing the empirical relationship on uncorrected quantities, as discussed in the Technical Note on Processing Algorithms [version as of June 2016]. For the C-130, the error in the measurement of ambient or static pressure (Δp) was found to be given by the following empirical representation, to an uncertainty of less than 0.3 hPa:

$$\frac{\Delta p}{p} = a_0 + a_1 \frac{\alpha}{a_r} + a_2 M \tag{1}$$

where p is the uncorrected measurement of pressure (PSFD or PSFRD), α is the angle of attack (AKRD), calculated from uncorrected measurements as described in the Algorithms document, a_r is a constant with value 1° (included only to keep the equation dimensionless), and M is the Mach number calculated from uncorrected measurements of static and dynamic pressure. The coefficients are $\{a_0, a_1, a_2\} = \{-0.00637, 0.001366, 0.0149\}$ for PSFD and $\{-0.00754, 0.000497, 0.0368\}$ for the alternate pressure measurement PSFRD. These coefficients were based on measurements collected during the IDEAS project of November 2011. They appeared to work well for many subsequent projects, as judged by consistency with the avionics-provided pressure PS_A. A representative example from the FRAPPE measurements is shown in Fig. 9.

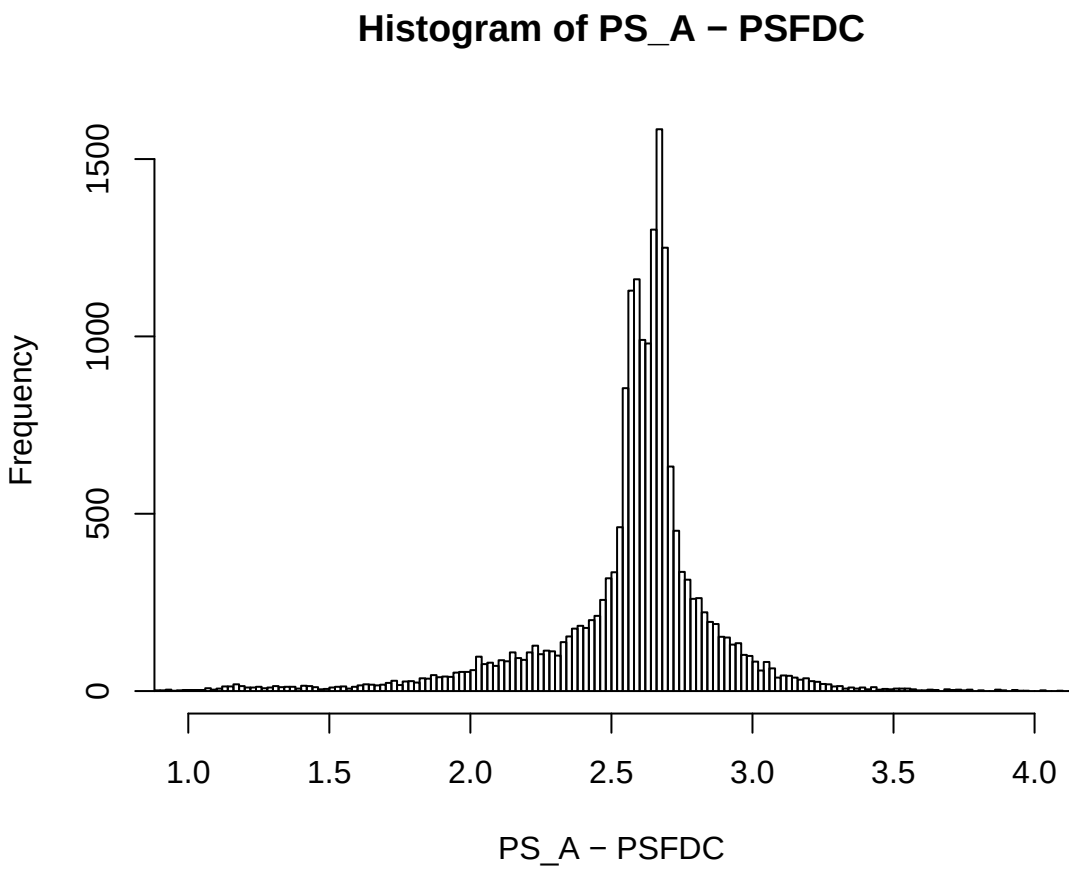

Figure 9: The difference between the avionic-provided pressure (PS_A) and the standard pressure after the correction as expressed in (1) (PSFDC).

The mean offset between the avionics-supplied pressure and the research pressure is 2.6 hPa, a value that is similar to those measured in other projects including NOMADSS, WINTER, and ARISTO-2015. It appears that the pressure correction is providing consistent results for recent C-130 projects. Further evidence is provided by a comparison of airspeed as measured by the LAMS and the conventional system employing the above PCOR function, as shown in Fig. 10. The mean difference between the LAMS-measured airspeed and the standard airspeed was 0.35 m/s and the standard deviation for 1-Hz measurements was 0.23 m/s. Because the LAMS-derived airspeed is smaller, even this small difference might arise from some airflow distortion at the displaced positions of the LAMS beams. There is some additional evidence for this in the next section.

These checks indicate that the usual PCOR function is working well for this C-130 project. The weakness is the available calibrations, present also in ARISTO-2015, is that measurements at altitudes between sea level and about 850 hPa have not been available. Problems may arise with use of the PCOR function as expressed in (1) to such low-level flight, so it will be important to revisit the

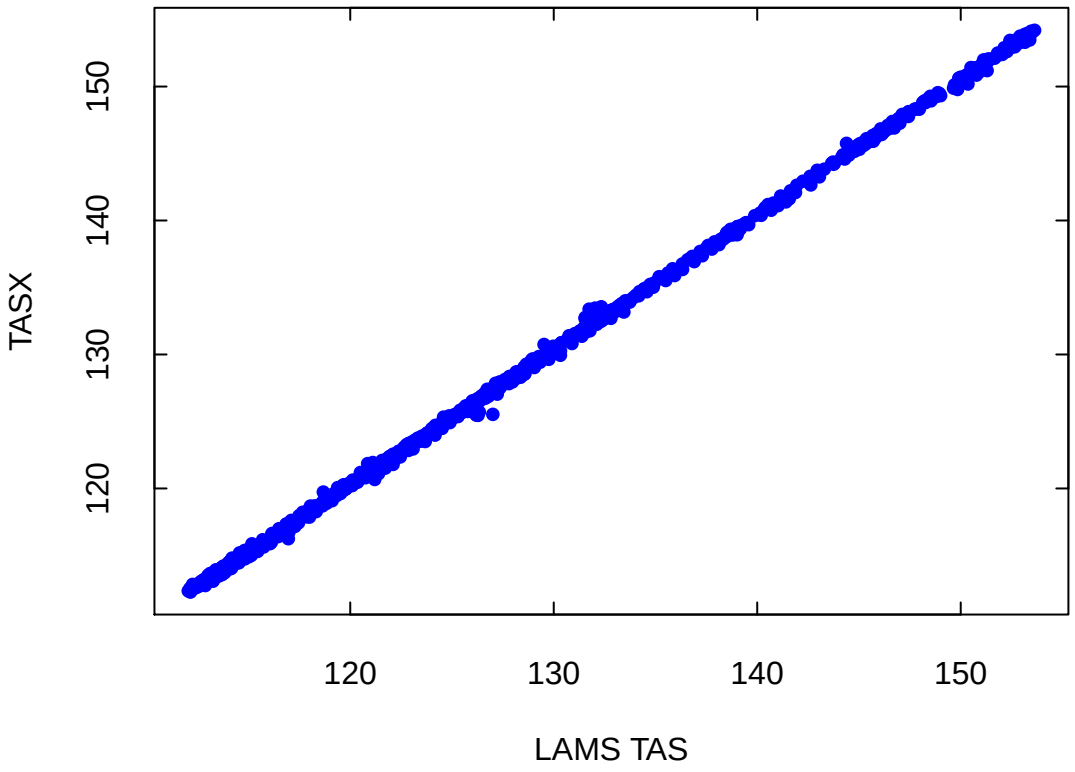

Figure 10: The conventional measurement of airspeed (TASX) plotted vs. the LAMS-derived measurement of airspeed (TASL), for speed run #7.

determination of the empirical relationship for the static defect once such low-level measurements are available.

LAMS-based measurement of temperature

Theory and data available

It was demonstrated in Cooper et al. (2014) that the LAMS-measured airspeed v_L can be used to measure the temperature in a way that is independent of any temperature sensor. One important aspect of this is that v_l, combined with the measurements of total pressure (p_t) and of ambient pressure (p), might provide a valid measurement of temperature in clouds. This independent measurement of temperature arises from the relationship between temperature and the speed of sound,

because the Mach number (M) can be determined from the measurements p_t and p so the speed of sound can be found from v_L/M. That measurement of temeperature will be explored in this section.

The equation leading to temperature, Eq. (24) in Cooper et al. (2014), is

$$T = \frac{v_l^2}{2c_p\left[\left(\frac{p_t}{p}\right)^{R_a/c_p} - 1\right]} \tag{2}$$

where T is the temperature on an absolute-temperature scale, c_p is the specific heat of air at constant pressure, and R_a is the gas constant for air. For a selected region with strong LAMS signals in clear air, the resulting temperature (converted to °C) was on average 1.4°C lower than the standard temperature ATX. However, this result is very sensitive to v_L and increasing v_l by 0.35 m/s (the measured difference between v_L and TASX) completely removed the offset. That may be an indication that the airspeed from LAMS shows a small effect from airflow distortion even though the beams are displaced XXX m ahead of the instrument.

To investigate the performance of this measurement of temperature in cloud, the in-cloud measurements from ARISTO-2015 were examined. The in-cloud measurements included those in the following table, along with a few other brief passes through rain, ice, or cloud:

flight	start	end	nature of cloud	performance of LAMS
1	173000	173800	warm, no 2D	mostly NG
1	174145	174600	warm, no 2D	maybe OK
1	184740	184830	only 2D; cold	OK
2	173000	192000	warm; high 2D	sporadic, weak
3	181000	182000	repeated cloud, warm	questionable, maybe OK
3	200900	201000	short, warm cloud	LAMS good
4	171500	172500	cold, ice	LAMS mostly OK
4	173000	174500	cold, ice	Beam1 NG, others weak
5	170600	171100	near 0C, short	Beam2 OK; Beam1 gaps
5	182200	182400	2D only; cold	LAMS NG

Case 1: Flight 3, 20:09:00 to 20:10:00

Flight 3, 20:09:00 to 20:10:00, is a short pass through a warm cloud with no ice or rain. Close inspection of the forward-pointing beam (beam 2) indicates that there are a few bad points in the center of this cloud, at times 20:09:48, 20:09:51. and 20:09:54, so these were set missing and then interpolation was used to fill in missing points in this time period.[3] The mean difference between airspeed determined in the conventional way and airspeed from LAMS was 0.55 m/s, consistent

[3]Beam 2 appeared to be affected in cloud more than the other beams, perhaps because of water striking and remaining on the forward-pointing aperture more than on the other beams pointing 35° from the forward direction.

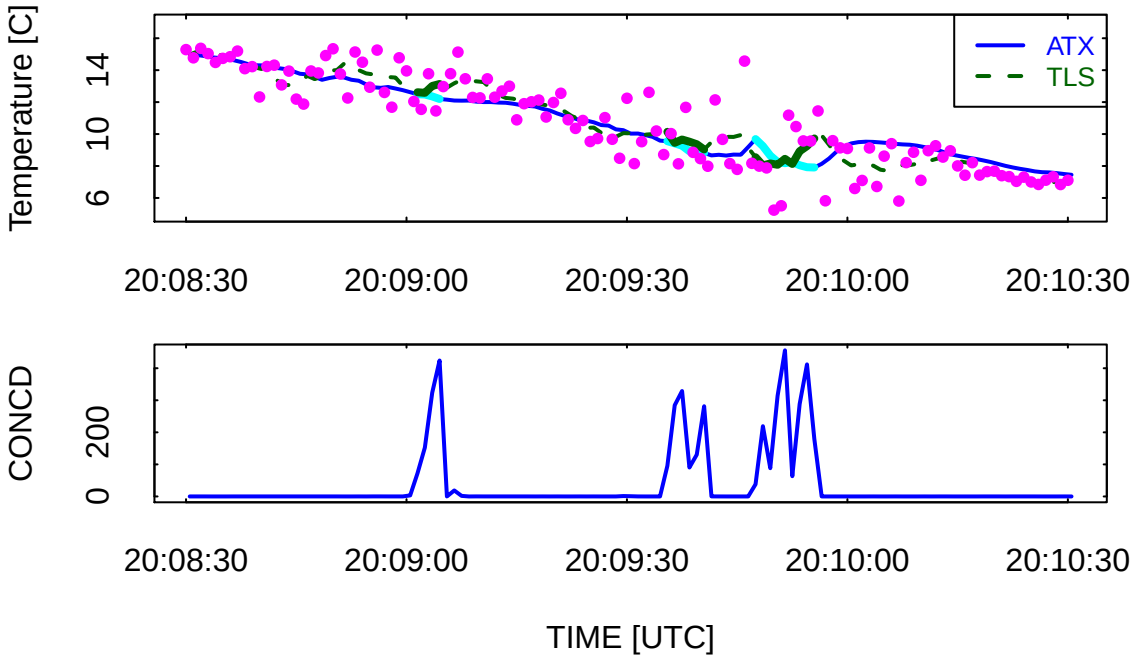

Figure 11: The temperature deduced from the measurement obtained using the LAMS-measured airspeed (magenta dots), adjusted as described in the text, and plotted with a smoothed version (TLS) and with the standard measurement of temperature (ATX). The measurements from periods where the CDP concentration exceeded 5_cm^{-3} are shown as thicker lines plotted, in the case of ATX, in a different color.

with the value found in the clear-air flight segment used in the preceding paragraph. To make it easier to judge differences produced by the cloud, this mean value was added to the LAMS-measured airspeeds and then smoothing over approximately a 5-s period was applied to the temperature calculated from the LAMS airspeed. The resulting temperature measurement for the cloud pass is shown in Fig. 11, where the magenta-colored points are the unsmoothed measurements of temperature. The unsmoothed measurement is quite noisy, so smoothing is important in order to see trends.[4]

[4]ATX is not smoothed, but it is thought to have a response time between 2 and 3 s.

Despite the noisy signal, particularly in the vicinity of the clouds, the LAMS-based temperature shows good correlation with the standard temperature. There is also a suggestion of a trend in the cloud passes: As the cloud pass proceeds, ATX tends to become lower relative to TLS. Because of the variability present, this is only suggestive, but there is some match to what would be expected if the ATX sensor (in this case, a HARCO anti-iced sensor) becomes wet in cloud because in that case evaporative cooling from the element in the dynamically heated and therefore <100%-humidity air in the housing causes an error of negative sign.

Case 2: Flight 2, 17:30:00–19:20:00

Next, the long cloud pass from flight 2 was examined. These measurements were from a low-level flight leg (near 7000 ft) at high temperature, >10°C, and there were high concentrations of particles measured by the 2DC. The LAMS-measured line-of-sight speeds were not always reliable,but it was possible to select regions of strong and apparently consistent signals from this long cloud pass. CDP-measured concentrations were often several hundred cm^{-3}, and 2D-measured concentrations ranged from 1–100 L^{-1}.

As was the case for the flight-3 case examined above, beam 2 appears to be more noisy than the other beams, and there are some cases where beam 1 (looking downward) appears to be affected by returns from the ground. Because the measurement of airspeed is over-constrained in the case of valid measurements from four beams, it is possible to use a chisquare test of consistency among the four beams as a test of validity of the solution. The chisquare for the solution was developed in the LAMSprocessing4Bwind.pdf memo:

$$\chi^2 = \sum_i \frac{(a_i' - a_i)^2}{\sigma^2} \tag{3}$$

where a_i' are the line-of-sight airspeeds measured in the four beams and a_i are the corresponding airspeeds determined using the direction-cosine matrix for the four beams and the best-fit result for the vector wind. For the four-beam case, the solution for the vector wind is

$$\mathbf{v} = \mathbf{M}\mathbf{a}' \tag{4}$$

and

$$\mathbf{a} = \mathbf{S}\mathbf{v} \tag{5}$$

where **M** and **S** are given by Eqs. 9 and 2 from that earlier memo. The solution to (3) is then given by

$$\chi^2 = \frac{1}{\sigma^2} \sum_i (a_i' - S_{ij} v_j)^2 \tag{6}$$

Code to calculate this value, using σ=1, is included in the "ProcessWind()" function in this code. For the region from flight 3 shown in Fig. 11, the mean value was 0.16 $m^2 s^{-2}$, so these 4-beam measurements were reasonably consistent, but there were five outliers with values exceeding 1 $m^2 s^{-2}$

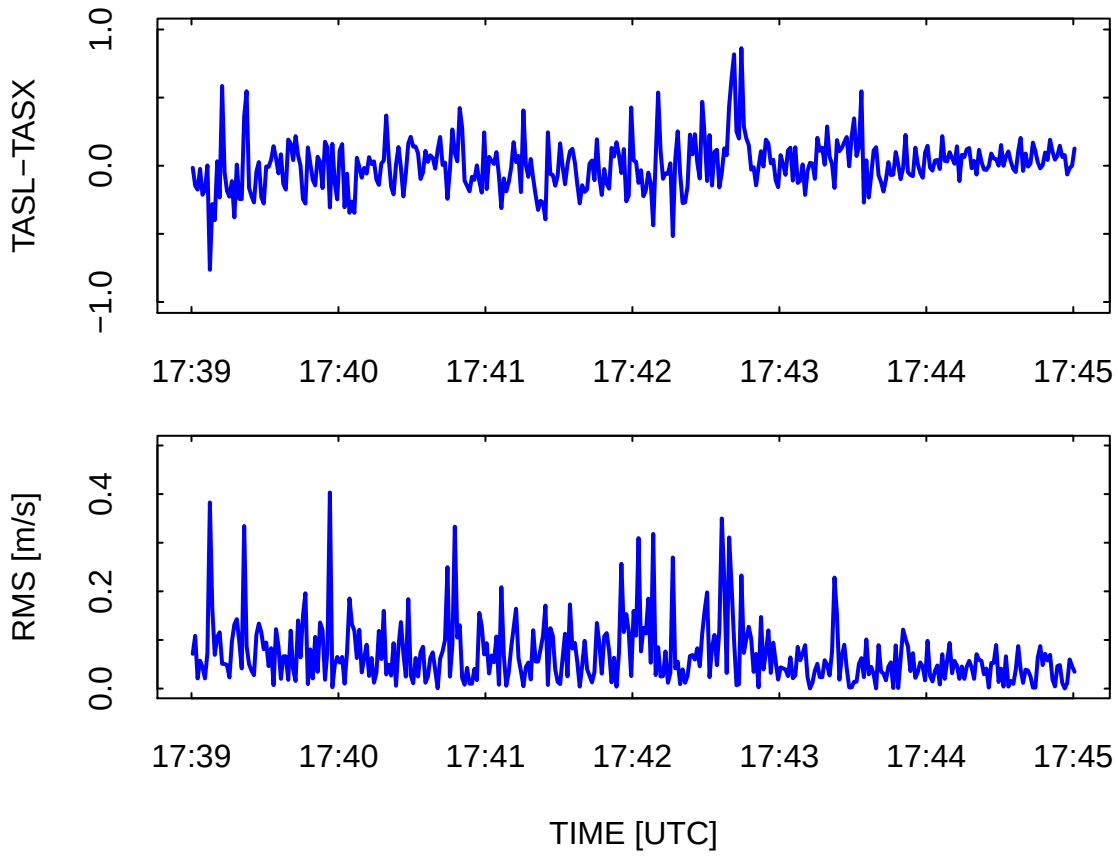

Figure 12: (top) The difference between the LAMS-derived airspeed (TASL) and the conventional airspeed (TASX), for the period from 17:39:00–17:46:00 from ARISTO-2015 flight 2. (bottom) The RMS error for the fit to the four measured line-of-sight beam speeds, for the same flight segment.

that should be excluded as being inconsistent among the four beams. The value of χ^2 can thus be used to identify regions where the 4-beam solution is questionable, and a requirement that it be smaller than about 0.5 m^2s^{-2}appears reasonable on the basis of values from good flight segments.

Figure 12 shows a segment from this flight for which the measurements appear consistent among the four beams, especially for the last 2-min period that is not in cloud. This flight segment was selected because the LAMS measurements are mostly consistent with the standard airspeed and have low RMS. Figure 13 shows the corresponding measurements of temperature from the two sources and also the droplet concentration. The in-cloud LAMS temperature is on average slightly lower than the standard temperature, by about $-0.21°$C, while the out-of-cloud measurements are offset in the other direction, with a mean difference of $0.17°$C. There is some correlation between the temperature difference and the liquid water content, as shown in Fig. 14. The observed

difference is in the opposite direction to that expected if ATX is cooled as a result of wetting of the sensor, so this result is not an indication of sensor wetting. An alternate explanation might be that the returned signal has greater contributions from locations closer to the LAMS in the high-backscatter of a cloud, so that the airspeed and hence temperature is biased low in such a region, with the bias increasing with the density of the cloud.

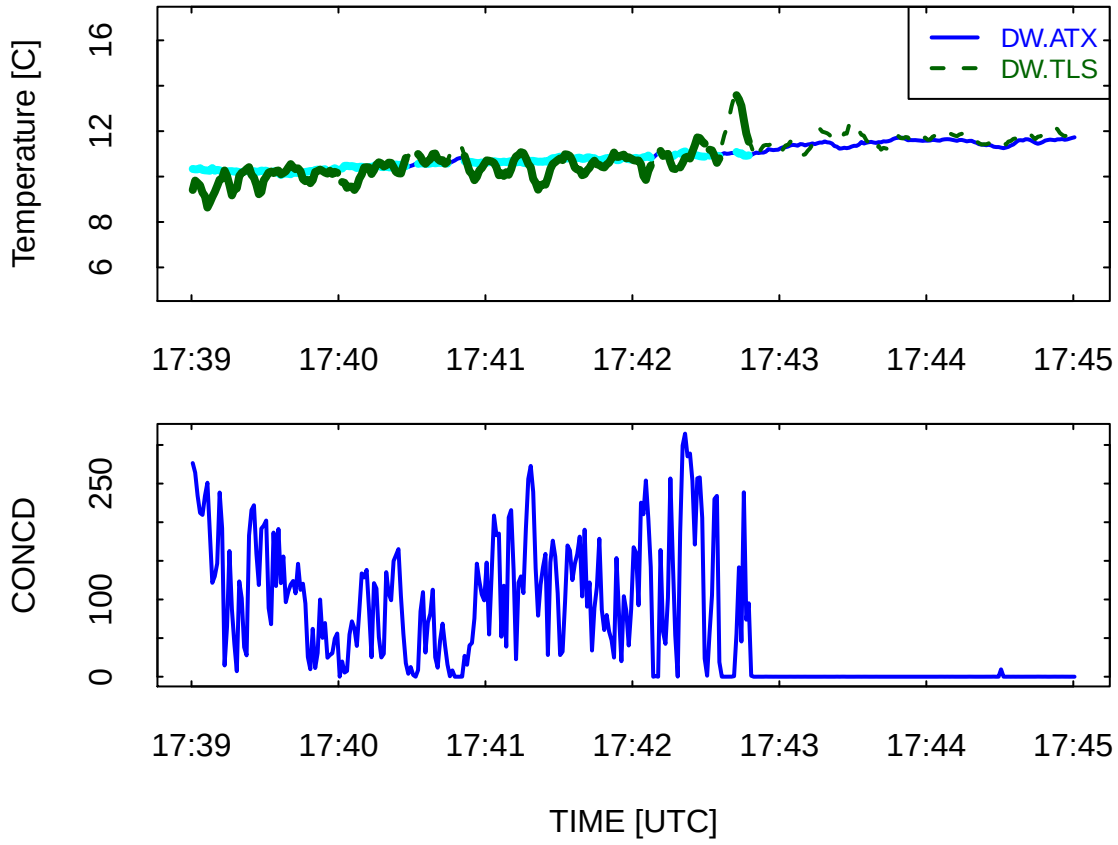

Figure 13: For the same flight period shown in the previous figure, the temperature deduced from the measurement obtained using the LAMS-measured airspeed (dark green line), adjusted as described in the text, plotted with the standard measurement of temperature (ATX). The measurements from periods where the CDP concentration exceeded 5_cm^{-3} are shown as thicker lines plotted, in the case of ATX, in a different color.

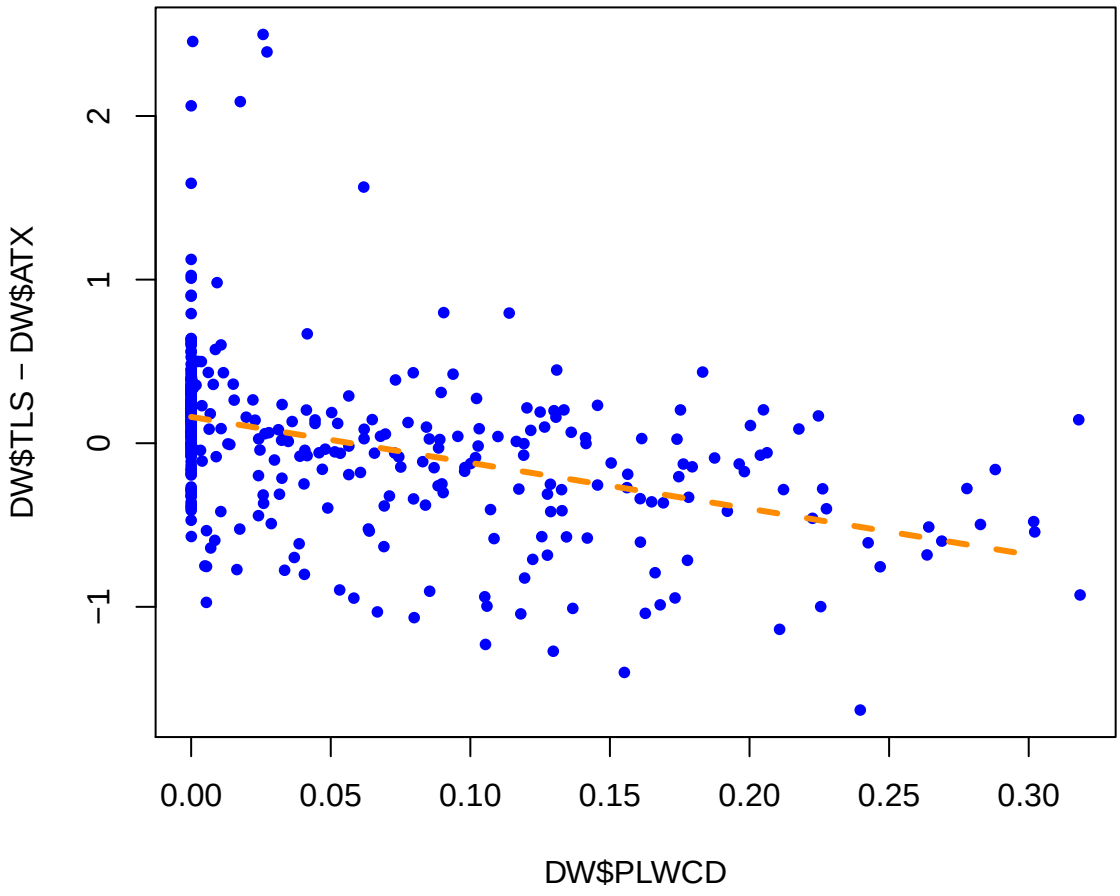

Figure 14: Dependence of the difference between the LAMS-derived temperature (TLS) and the standard temperature (ATX) as a function of the liquid water content measured by the CDP (PLWCD), for the same flight period shown in the preceding two plots.

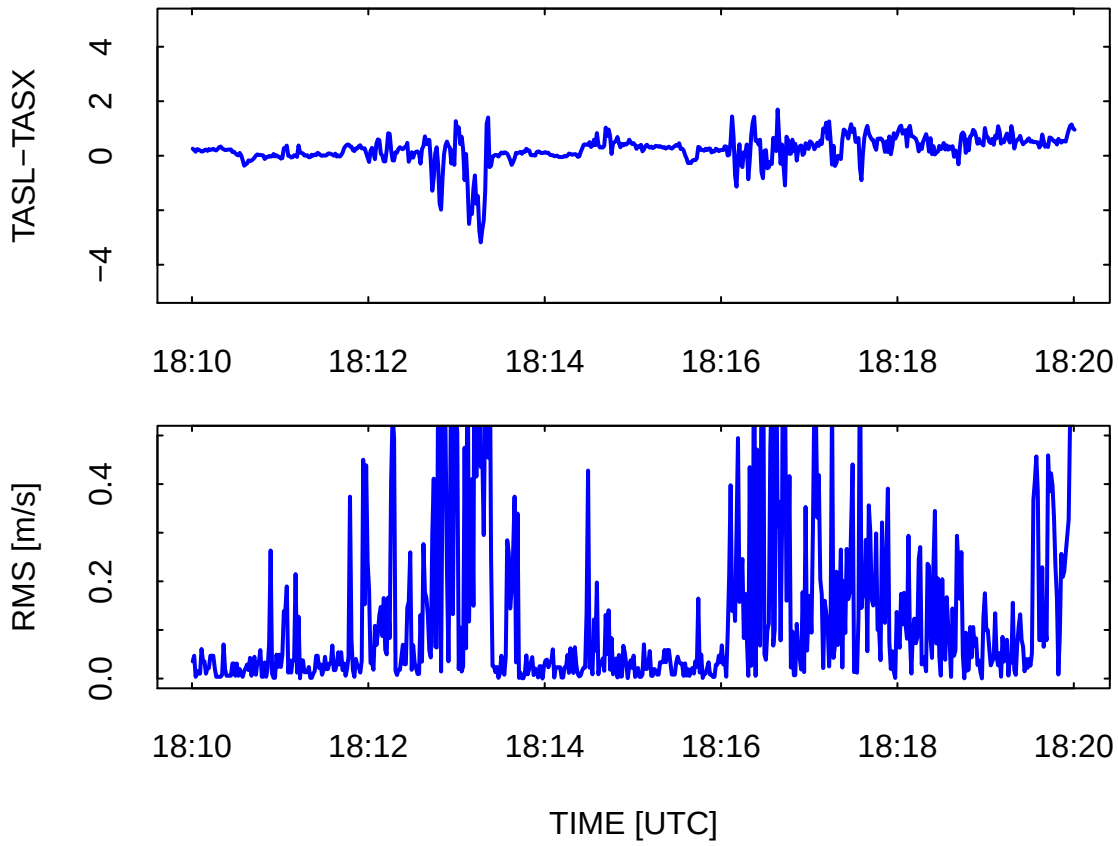

Figure 15: (top) The difference between the LAMS-derived airspeed (TASL) and the conventional airspeed (TASX), for the period from 18:10:00–18:20:00 from ARISTO-2015 flight 3. (bottom) The RMS error for the fit to the four measured line-of-sight beam speeds, for the same flight segment.

Case 3: Flight 3, 18:10:00–18:20:00

The third case examined here is a series of passes through clouds at temperatures near freezing. Droplet concentrations were often several 100/cm^3, and there were 2D particles often in concentrations of 1–10/L. The cloud pass near 18:13 was a more dense cloud than those presented above, with droplet concentrations around 400 cm^{-3} and liquid water content above 0.6 g m^{-3}. It serves as a good illustration of the problems with LAMS that occur in a dense cloud. The measurements of airspeed and the associated RMS for this flight period is shown in Fig. **??**, and the associated measuirement of temperature for the pass through particularly dense cloud is shown in Fig. 16. In this dense cloud, the RMS for the four-beam measurements became >0.5 inside the cloud, the LAMS-measured airspeed was about 2 m/s below the conventional measurement, and as a result the LAMS-measured temperature was as much as 10°C below the standard temperature ATX.

However, this large error arose mostly from beam 2, which alone would give an error of more than 30°C. If instead airspeed is determined using the three beams slanted into the wind by about 35°, the result (plotted as TLS3, the orange line in Fig. 16) shows a smaller but still significant negative bias relative to ATX. This shows the value of using four beams and applying an RMS test to exclude bad measurements, because the measurements were quite seriously biased in this dense cloud and only this RMS test was able to identify the regions where measurements are unreliable.

Figure 17 shows a similar plot for a subsequent period of flight through this sequence of small clouds. The temperature based only on beam 2 is again strongly affected and evidently too low in this sequence of weaker clouds. However, it has less influence on the 4-beam solution, and both the 4-beam and the 3-beam solution appear reasonable. The difference between the 3-beam solution (TLS3) and ATX is 0.3°C for locations out-of-cloud but 0.48°C for in-cloud measurements. Because errors in the LAMS-derived temperature are negative when influenced by cloud, these differences suggest possible evaporative-cooling influence on the standard temperature probes.

Conclusions, LAMS-measured temperature

The three cloud regions discussed in the previous three subsections are the best measurements from ARISTO-2015 for this study. The following assessment is based on those studies:

1. The temperature deduced from LAMS is mostly valid out-of-cloud. Because it is only dependent on the LAMS-deduced airspeed and on the Mach number that is in turn based on ambient and dynamic pressure, themselves calibrated by the LAMS measurements, and it does not rely on any temperature sensor beyond that needed for the initial calibration. The LAMS-derived temperature therefore can be a useful check on the performance of standard temperature sensors and may be useful in flagging problems with those sensors. However, the LAMS-based measurement of temperature is noisy, especially in turbulence, so averaging over periods of at least 10 s or more appears necessary.

2. When in cloud, beam 2 is often strongly biased toward negative temperature because the measured airspeed appears to be too low. The problem does not appear as strongly in the other three beams, perhaps because they are at a 35° angle to the relative wind. Possible causes are water on the forward surface that causes defocusing of the beam or strong scattering or multiple scattering that displaces the effective sample volume closer to the aircraft into distorted airflow. The temperature measurement based on a single forward-pointing beam therefore is not useful in cloud.

3. The RMS for the four-beam solution for airspeed is a valuable indicator of quality, and it often flags regions with bad measurements when both available processing schemes for the LAMS line-of-sight velocities otherwise indicate good measurements. This benefit from the 4-beam configuration was not anticipated but appears to be a particularly important reason for using that configuration.

4. The airspeed based on the three off-axis beams is much less affected by cloud and appears to provide a valid measurement except in very dense cloud. The temperature deduced from that measurement of airspeed tends to be slightly higher than the standard measurement in warm cloud, as would be expected if there is evaporative cooling as a result of wetting of the temperature sensor. However, this conclusion is based on only a few cloud passes, and more data and analysis would help test the utility of this measurement.

5. It would be especially useful to operate a 4-beam LAMS with the in-cloud radiometer and perhaps an unheated temperature sensor to obtain further tests of the LAMS-based temperature measurement.

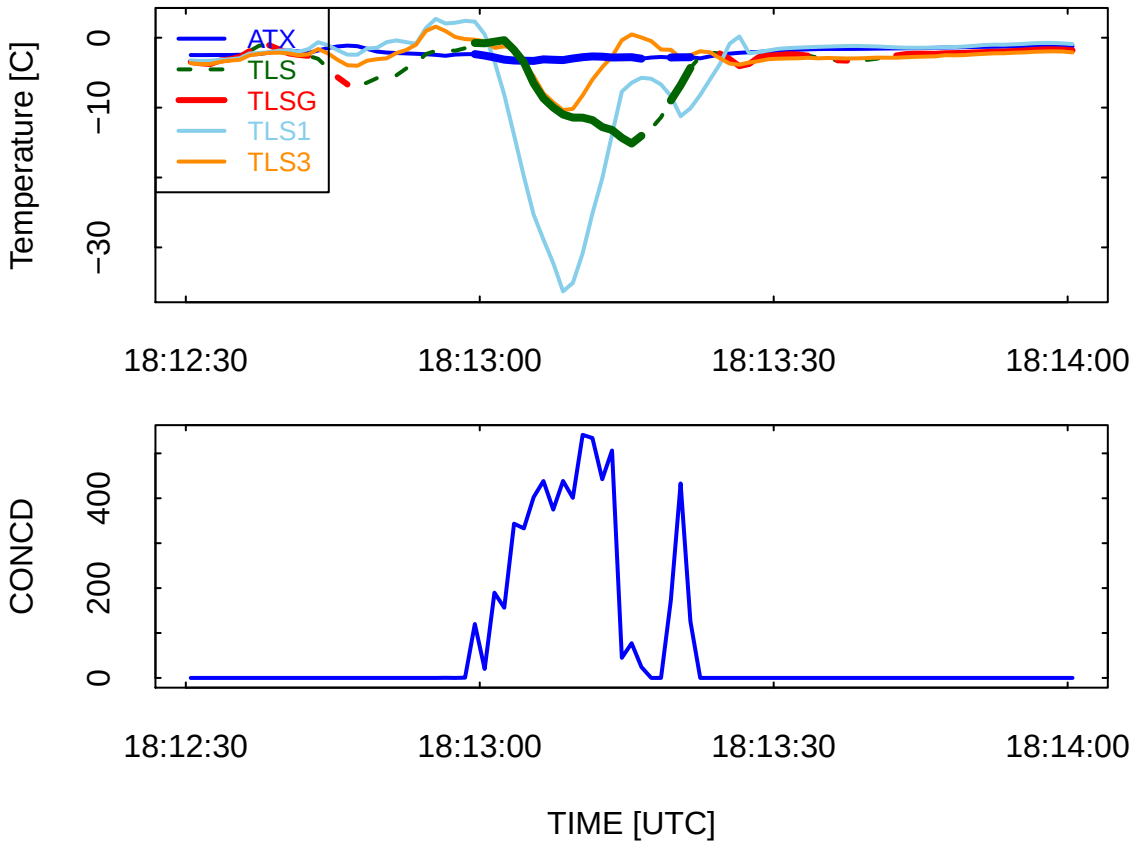

Figure 16: For the subset of the flight period shown in the previous figure from 18:12:30–18:14:00, the temperature deduced from the measurement obtained using the LAMS-measured airspeed (TLS, dark green line), adjusted as described in the text, plotted with the standard measurement of temperature (ATX). The measurements from periods where the CDP concentration exceeded 5_cm^{-3} are shown as thicker lines. The red line on this plot (TLSG) shows the periods where TLS was based on measurements with RMS smaller than 0.2 m/s. The cyan line (TLS1) is the result based only on the forward-pointing beam 2, and the orange line (TLS3) is the result based on the 3-beam result using beams 1, 3, and 4.

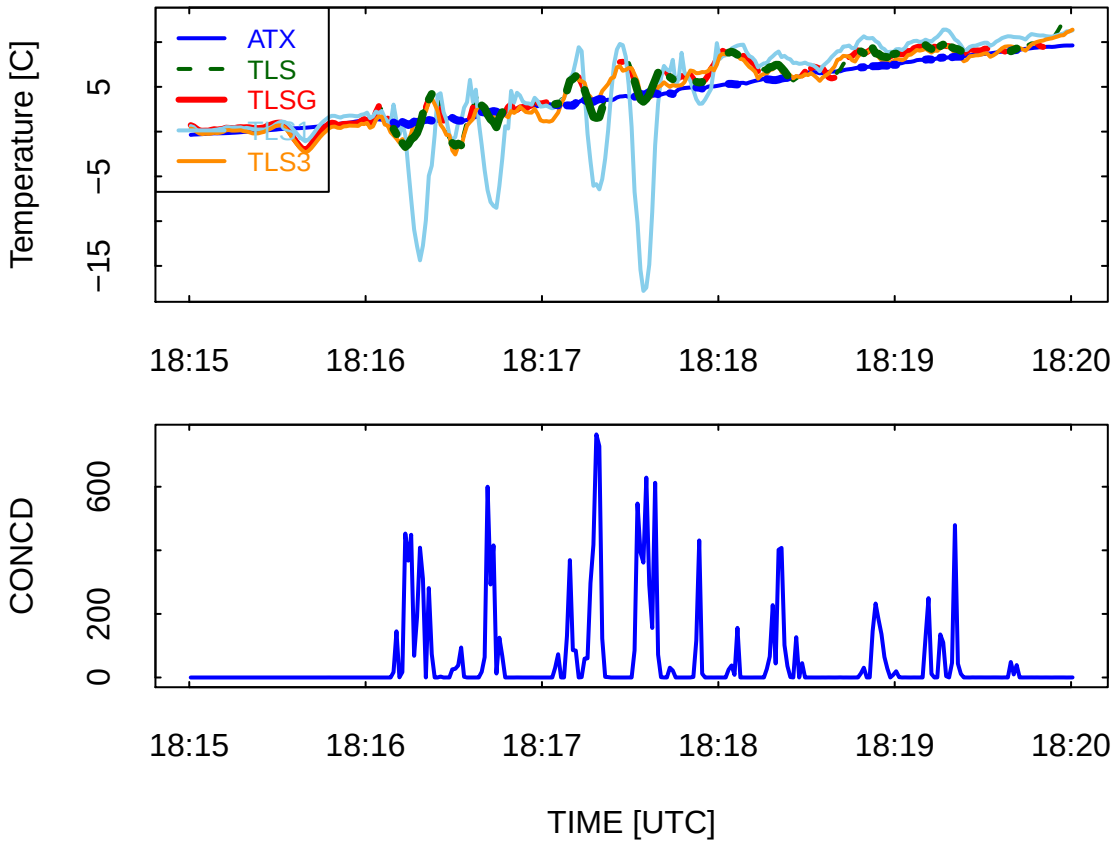

Figure 17: Same as in the previous plot, but for a later portion of the flight segment. See the caption for the previous plot.

Transient effects on wind measurements, C-130

Transient effects on measurements of vertical wind were discussed for the GV in this earlier memo. The conclusion of that memo was that effects, while detectable and correctable, were at the margin of uncertainty for wind measurements and so had little significant effect on wind measurements from the GV. A similar study is not possible here because there wasn't a good pitch maneuver to use for this purpose. Two good maneuvers were flown in flight 4, 18:21:00–18:26:00 and 18:58:00–19:01:00, but in each case the LAMS signals were inadequate to provide a good measurement of vertical wind, as needed for this study. Other pitch maneuvers were flown, but some were compromised by times when the LAMS IRU was not working or, in the last flight, when LAMS signals were too weak. This study will have to await better measurements, perhaps from ARISTO-2016.

– End of Memo –

Reproducibility:

PROJECT:	ARISTO2015-LAMS
ARCHIVE PACKAGE:	ARISTO2015-LAMS.zip
CONTAINS:	attachment list below
PROGRAM:	ARISTO2015-LAMS.Rnw
ORIGINAL DATA:	
WORKFLOW:	WorkflowARISTO2015-LAMS.pdf
GIT:	https://github.com/WilliamCooper/ARISTO2015-LAMS.git

Attachments: ARISTO2015-LAMS.Rnw
ARISTO2015-LAMS.pdf
ARISTO2015-LAMS.Rdata.gz
SessionInfo